LCC-0139
SLAC-TN-04-042
May 2004

Linear Collider Collaboration Tech Notes

Alternative Main Linac BNS Configurations for Reduced Energy Spread

Andrei Seryi and Peter Tenenbaum

May 2004

Stanford Linear Accelerator Center
Stanford University
2575 Sand Hill Road
Menlo Park, CA

Abstract: We present a series of alternate BNS phase configurations for the 500 GeV CM NLC main linac in which the energy spread at the end of the linac is reduced from its nominal 0.25% value. The energy spectrum, achievable IP beam energy, energy bias, and linac stability are evaluated for the alternate cases. We conclude that the RMS energy spread and energy bias in the NLC can easily be reduced but that modest reductions in CM energy are required.

Work supported by the Department of Energy Contract DE-AC03-76SF00515

Alternative Main Linac BNS Configurations for Reduced Energy Spread

A. Seryi, P. Tenenbaum
LCC-Note-0139
May 24, 2004

Abstract

We present a series of alternate BNS phase configurations for the 500 GeV CM NLC main linac in which the energy spread at the end of the linac is reduced from its nominal 0.25% value. The energy spectrum, achievable IP beam energy, energy bias, and linac stability are evaluated for the alternate cases. We conclude that the RMS energy spread and energy bias in the NLC can easily be reduced but that modest reductions in CM energy are required.

1 Introduction

One of the key advantages of electron colliders over hadron facilities is that the energy distribution of the collisions is quite narrow. In hadron machines, the fact that the colliding particles are composite means that the energy of a given collision is determined not by the energy of the hadron but by the energy distribution of its constituent quarks and gluons. The best available evidence is that electrons are fundamental, which implies that the energy in a given collision is determined by some electrodynamic factors (initial state radiation and beamstrahlung) and by the energy of the electron and positron which collide with one another. The energy width of the latter is determined by the energy spread of the two beams at the collision point. Although the energy spread from beamstrahlung is larger than the design energy spread of present-day linear colliders, its effects can be measured using techniques such as Bhabha acolinearity analysis. This leave the IP energy spread of the incoming beams as the remaining quantity which must be controlled for physics purposes.

The NLC design parameters call for an RMS energy spread at the IP of about 0.25%, with a two-horned "batman" distribution as shown in Figure 1. This energy spread is sufficiently small from the point of view of the final focus energy bandwidth, but some particle physics studies can be improved through reduction in the IP energy spread. In this Note we study alternative configurations of the main linac which will allow a reduced RMS energy spread at 500 GeV CM.

1.1 Physics of Linac Energy Spread – Overview

There are a number of physical effects and proceses which have an impact on the ultimate energy spread of the NLC. These are briefly reviewed here.

1.1.1 Damping Ring and Bunch Compressors

The NLC main damping rings have a natural energy spread determined by the stochastic nature of radiation emission in a storage ring. For the NLC rings, this energy spread is 0.0975% [1]. The RMS bunch length in the rings is a function of the energy spread, the latttice momentum compaction, the ring's RF cavity voltage, and certain collective effects; for the NLC rings, the design bunch length is 5.5 mm RMS.

The first bunch compressor in the NLC reduces the RMS bunch length from 5.5 mm to 0.6 mm, and increases the energy spread by the same factor. In the process, the compressor performs a longitudinal phase rotation, causing a particle's offset in t on damping ring extraction to become an offset in δ after the compressor, and vice versa. The pre-linac and second bunch compressor

preserve this relationship as they compress the bunch to 0.110 mm RMS length. The RMS energy spread of a bunch at injection to the main linac is 1.48%, but at this location there is a small $t - \delta$ correlation such that the uncorrelated RMS energy spread is 1.28% or 101 MeV.

It is important to note that the 101 MeV uncorrelated energy spread at main linac injection cannot be corrected by any downstream system. It is in effect an irreducible energy spread, and is an absolute limit on the minimum achievable energy spread in the NLC. At 250 GeV per beam this is an energy spread of 0.04%, while at 45.6 GeV per beam it is 0.22%. It is also worthwhile to realize that a similar phenomenon sets the minimum achievable energy spread in TESLA. In the latter case the energy spread of 2.8% at main linac injection corresponds to 129 MeV, yielding a modestly larger "floor" to the achievable energy spread as compared to the NLC.

1.1.2 RF Curvature and Beam Loading Compensation

If the RMS bunch length is a significant fraction of the RF wavelength used to provide acceleration, the sinusoidal variation in voltage over the bunch length will cause the head and tail of the bunch to receive less acceleration than the core, leading to additional energy spread. In the NLC case the RMS bunch length is 110 μm while the RF wavelength is 2.63 cm. For a bunch accelerated near the RF crest, the droop of the voltage over the bunch length is therefore on the order of 10^{-5}. This will clearly cause a negligible energy spread compared to the aforementioned 101 MeV from the bunch compressors.

A more significant source of energy spread is single-bunch beam loading in the RF structures. This loading causes the particles in the beam tail to receive less acceleration than particles in the head, resulting in an energy spread. The loading voltage along the bunch from the NLC main linac structures is shown in Figure 2.

This energy spread can be partially compensated by running off-crest in the linac, so that the slope of the RF sinusoid opposes the slope of the loading. Because the loading is a nonlinear effect (the diffuse head and tail experience almost no loading, while the dense core is heavily loaded), but the off-crest running produces a near-linear variation in energy, the compensation is not complete. Typically the energy spread of the beam core is compensated but the energy spread of the head and tail is worsened, and these two contributions are traded off against one another. Even more vexing is that off-crest acceleration reduces the total beam energy which can be achieved. The NLC runs about 11° off-crest on average to achieve its 0.25% RMS energy spread, leading to a 1.6% reduction in achievable main linac acceleration. In the NLC case, for example, the loading compensation is not complete – the energy in the tail is allowed to be somewhat lower than the energy in the head, since full compensation would require sacrificing additional voltage.

1.1.3 BNS Damping

The strong wakefields in the NLC linac would ordinarily cause unacceptable emittance dilution in the presence of beam jitter, by amplifying the jitter of the tail of each bunch relative to the head. This effect is mitigated by the use of BNS damping: introducing a correlated energy spread such that the wakefield kick experienced by the tail of the beam is cancelled by the chromaticity of the focusing lattice [2]. Since a bunch with a positive offset deflects the tail in the positive direction, the countervailing effect of the lattice must produce a negative kick for a positive offset – that is, the tail must be over-focused relative to the head. This in turn implies that the energy of the tail should be lower than the energy of the head.

At the end of the NLC main linac, the energy spread required to achieve BNS damping locally (in which the deflections from wakefields and the deflections from the quads cancel one another over the length of a single FODO cell) is larger than what can be comfortably accomodated by

the final focus. The competing requirements of BNS damping and energy spread in the final focus are addressed by introducing a relatively large energy spread in the upstream end of the linac, maintaining the large energy spread through most of the linac, and then removing most of it prior to entry into the final focus. This is achieved by running the beam a few degrees behind the RF crest in the upstream reaches of the linac, and allowing the combination off-crest running and beam loading to create the desired energy spread; running slightly ahead of the crest in the middle of the linac, so that beam loading and off-crest operation nearly cancel and the RMS relative energy spread remains nearly constant; and running the beam ahead of the crest in the downstream end, to compensate beam loading and remove the correlated energy spread used for BNS damping. Figure 3 shows the design BNS phases and RMS energy spread in the NLC main linac. Figure 4 shows the emittance growth along the linac for a 1 σ_y injected offset with the design BNS configuration.

Note that the use of BNS damping increases the RMS phase angle of the RF with respect to the beam, and thus decreases even further the acceleration available in the linac. In the case of the design BNS configuration, a total of 259 GeV installed voltage is needed to achieve acceleration from 7.87 GeV to 250 GeV, a "voltage tax" of about 7% for BNS damping and beam loading compensation combined.

2 Reducing the IP Energy Spread

Given the sources of energy spread discussed above, the key to reducing the energy spread at the end of the linac is to more fully compensate the single-bunch beam loading. This can be achieved by running the beam ahead of the RF crest for a greater length of the linac, or by increasing the distance between the RF crest and the beam in the section where the beam is ahead of the crest, or both. In this study, the energy spread was decreased by increasing the fraction of linac used to take out the energy spread while limiting the maximum phase angle to 30°, as in the design BNS configuration. In practice, the energy at which the linac switches from near-crest (1° off-crest) to 30° off-crest was decreased in steps from the nominal 170 GeV to as low as 75 GeV.

Figure 5 shows the energy spectrum of the beam at the end of the linac as a function of the aforementioned final switch energy. As expected, the energy spread of the core is reduced for earlier switch points, while the energy spread in the tails is larger. In all cases, the resulting total energy spread of the beam can be accomodated by the aperture of the energy collimator in the beam delivery system, and all particles in the bunch pass through the IP without producing backgrounds.

Figure 6 shows the full-width at half-maximum of the bunch as a function of final switch energy. In the case of two-horned distributions the value used for the maximum is the mean of the maxima of the two horns. For comparison, in the case of TESLA the positron beam has an RMS energy spread of approximately 0.07% while the electron beam's energy spread is increased to 0.14% by synchrotron radiation in the undulator used for positron production. Conveniently both the arithmetic and the geometric mean work out to about 0.1% RMS or 0.235% FWHM, comparable to the NLC using a switch point of 100 GeV to 105 GeV.

Figure 7 shows the total linac voltage required to achieve 250 GeV at the end of the linac, as a function of final switch energy. As expected, the voltage requirements are greater for earlier switch points, indicating that either total voltage or final energy must be traded off against energy spread.

Besides voltage requirements, the other drawback to reduced final energy spread is that the BNS compensation of wakefield emittance growth is weakened. Two methods were used to quantify this weakening. The first method was to calculate the emittance versus s position along the linac for each BNS configuration, assuming a 1 σ_y initial offset of the beam. The other was to calculate the end-linac emittance for a 1 μm offset of various quads along the length of the linac. Note that this latter metric does not correspond to an actual situation which would be encountered in

operation: under normal operational conditions, moving a quadrupole would launch a betatron oscillation which would then be corrected by downstream feedbacks, while in this study we have simply allowed the oscillation to propagate freely to the end of the linac. The point of this exercise is simply to quantify the sensitivity of the linac to disturbances, or its "touchiness," as a function of final switch energy.

Figure 8 shows the evolution of the beam emittance along the linac for a 1 σ_y initial offset. The four earliest switch points permit more emittance growth than the design, while the others all permit less growth. From this point of view, then, any switch point from 95 GeV can be accepted, and even 90 GeV is not drastically worse than the nominal 170 GeV point.

Figure 9 shows the emittance at the end of the linac for offsets of various quads along the length of the linac. While the nominal case (170 GeV final switch point) has the best performance in this study, the most sensitive quadrupoles for 120 GeV or 130 GeV final switch points are only a factor of 3 to 4 more sensitive than the most sensitive quads in the nominal case. We can therefore expect that operation in one of these modes will be moderately more difficult than in the nominal, and would benefit from a more aggressive scheme of steering feedbacks than is required for the nominal case. Another option would be to adjust the linac optics to improve the stability under conditions of reduced energy spread.

Given the increased sensitivity to quad offsets displayed in Figure 9, one might expect that the beam-based alignment of the main linac may converge to a less optimal solution for configurations which produce a lower energy spread at the IP. In a test, the tuning algorithm described in [3] was applied to the main linac in the nominal configuration and compared to the performance in the optimal configuration (with the final phase-switch at 120 GeV); in each BNS configuration 100 misaligned linacs were generated and tuned up. It was found that the mean emittance growth for the optimal configuration was about 0.5 nm larger than the mean growth for the nominal configuration. Note that 0.5 nm is about 2.5% of the 20 nm vertical emittance extracted from the damping ring, which is not a very large increment. This indicates that in practice the beam dynamics of the optimal configuration may be almost as tractable as those of the nominal configuration, although further study of feedbacks and performance over time are required to verify this.

3 Collisions with New BNS Configuration

In this section we will describe evaluation of the luminosity spectra and energy bias for these new BNS configurations.

For these evaluation we use IP beam distributions (files with saved (x,x',y,y',z,E) for each macroparticle in the bunch) obtained with tracking of several realistically misaligned NLC machines corresponded to the nominal BNS configuration (these are machine configurations used for TRC studies, when both NLC and TESLA were simulated by the same codes). The energy-Z dependences of these distributions were then modified so that the correlated energy spread would correspond to the new BNS configuration. The uncorrelated energy spread was not affected by this transformation, and the correlation between particle energy and particle horizontal angle (introduced by the nonzero η'_x at the NLC IP) is properly included. These new IP beam distributions were then used as an input to beam-beam program Guinea-Pig [4] to obtain luminosity spectrum and determine the so called energy bias. The energy bias is the error in the determination of the luminosity-weighted center of mass energy. It was found in [5] that the specific energy-z correlation in combination with beam-beam effects may cause this energy bias to vary from several hundred ppm (parts per million) up to about 1000 ppm. One of the goals of the considered new BNS configuration was to reduce this energy bias.

Figure 10 shows the energy bias and the rms width of the luminosity spectrum versus BNS final energy switch. One can see that the most optimal BNS configuration, which minimizes both the energy bias and the width of the luminosity spectrum, corresponds to the energy switch point of 120GeV. Interestingly, the final energy spread for this optimal switch point is somewhat larger than the minimum achievable energy spread. One can also see that the minimum is rather shallow – the range where the energy bias is smaller than 200 ppm is quite wide - this reduces sensitivity to parameters and makes it easy to set up such a low energy bias regime. In addition, the shallowness of the minimum implies that in normal operation one can set the final switch point to a somewhat lower energy which reduces the energy spread, or to a somewhat higher energy which reduces the total voltage required, while still preserving a narrow luminosity spectrum and small energy bias. It is also important to note that 120GeV energy switch configuration is as good as the nominal case in terms of the emittance growth for one sigma offset (see Figure 8) and only modestly more sensitive to quad offset in the linac (see Figure 9).

Figure 11 shows the energy versus longitudinal position within the bunch for one of the IP beam distributions for the nominal BNS and for the new optimal BNS.

Figure 12 shows luminosity spectra for six different IP beam distributions, for the nominal BNS and for the new BNS. One can see that luminosity spectra become more symmetrical, more gaussian-like and their dependence on the machine settings are reduced considerably.

Figure 13 shows luminosity spectra for NLC with nominal BNS and with new optimal BNS, in comparison with TESLA. One can see that the last two cases are very similar.

Figure 14 shows sensitivity of the energy bias to the vertical offset of the beams. This is an important figure of merit since this vertical offset will always have certain jitter. One can see that in NLC with new optimal BNS this sensitivity is reduced to the level below 100ppm which is about three times better than in TESLA where higher disruption causes higher variation of the energy bias.

4 Conclusion

We have studied the implications of reducing the IP energy spread in the NLC by increasing the fraction of the linac which is phased to remove the head-tail energy spread required for BNS damping. The FWHM energy spread can in this way be reduced from its nominal value of 0.9% to as little as 0.09%. Changing the linac configuration in this way requires additional RF voltage to achieve the design CM energy of 500 GeV, and introduces greater sensitivity to quadrupole offsets. In the most extreme cases the emittance growth from incoming betatron oscillations becomes unacceptable, but for the cases of interest this is not a problem.

When the properties of the collision are considered, it is found that the energy bias and luminosity spectrum are more optimal for a configuration in which the energy spread is somewhat larger than the minimum. At this optimal configuration linac operation will be moderately but not excessively more difficult than in the design configuration. The energy bias and luminosity spectrum in the optimal case are comparable to TESLA, and the sensitivity of the energy bias to the beam-beam offset at the IP is smaller than for the TESLA case. The width of the luminosity spectrum remains tolerably small for a range of configurations, and the energy bias is also small over this range. This gives the NLC the freedom during operation to maintain a narrow luminosity spectrum and small energy bias while optimizing other linac parameters.

In summary, the benefits of operation at reduced energy spread are quite attractive, and the drawbacks appear to be addressable. Some further study of the linac stability and tuning issues should be performed.

5 Acknowledgement

Without the input and assistance of T.O. Raubenheimer and N. Graf, this study would not have been possible.

References

[1] A. Wolski and M. Woodley, "The NLC Main Damping Ring Lattice," LCC-0113 (2003).

[2] V.E. Balakin, A.V. Novokhatsky, V.P. Smirnov, "VLEPP: Transverse Beam Dynamics," *Proceedings, High Energy Accelerators* (1988).

[3] P. Tenenbaum, "Main Linac Single Bunch Emittance Preservation in the NLC and US Cold LC Configurations," LCC-0137 (2004).

[4] D. Schulte, CERN-PS-99-14, 1999.

[5] M. Woods, K. Moffeit, T. Raubenheimer, A. Seryi, C. Sramek, A. Florimonte, "Luminosity, Energy and Polarization Studies for the Linear Collider: Comparing e+e- and e-e- for NLC and TESLA", SLAC-PUB-10353, 2004.

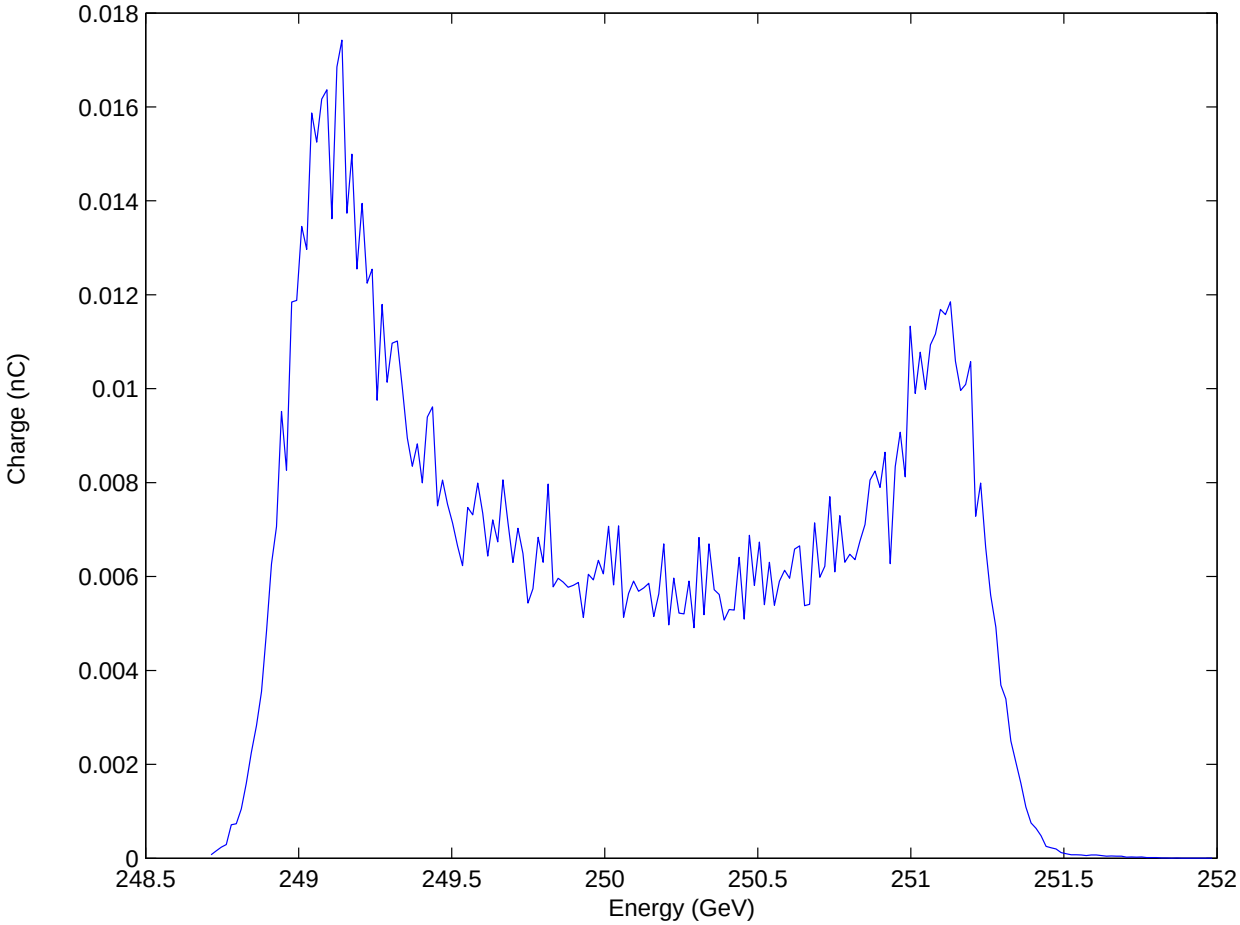

Figure 1: Spectrum of the beam at the end of the NLC linac for nominal conditions.

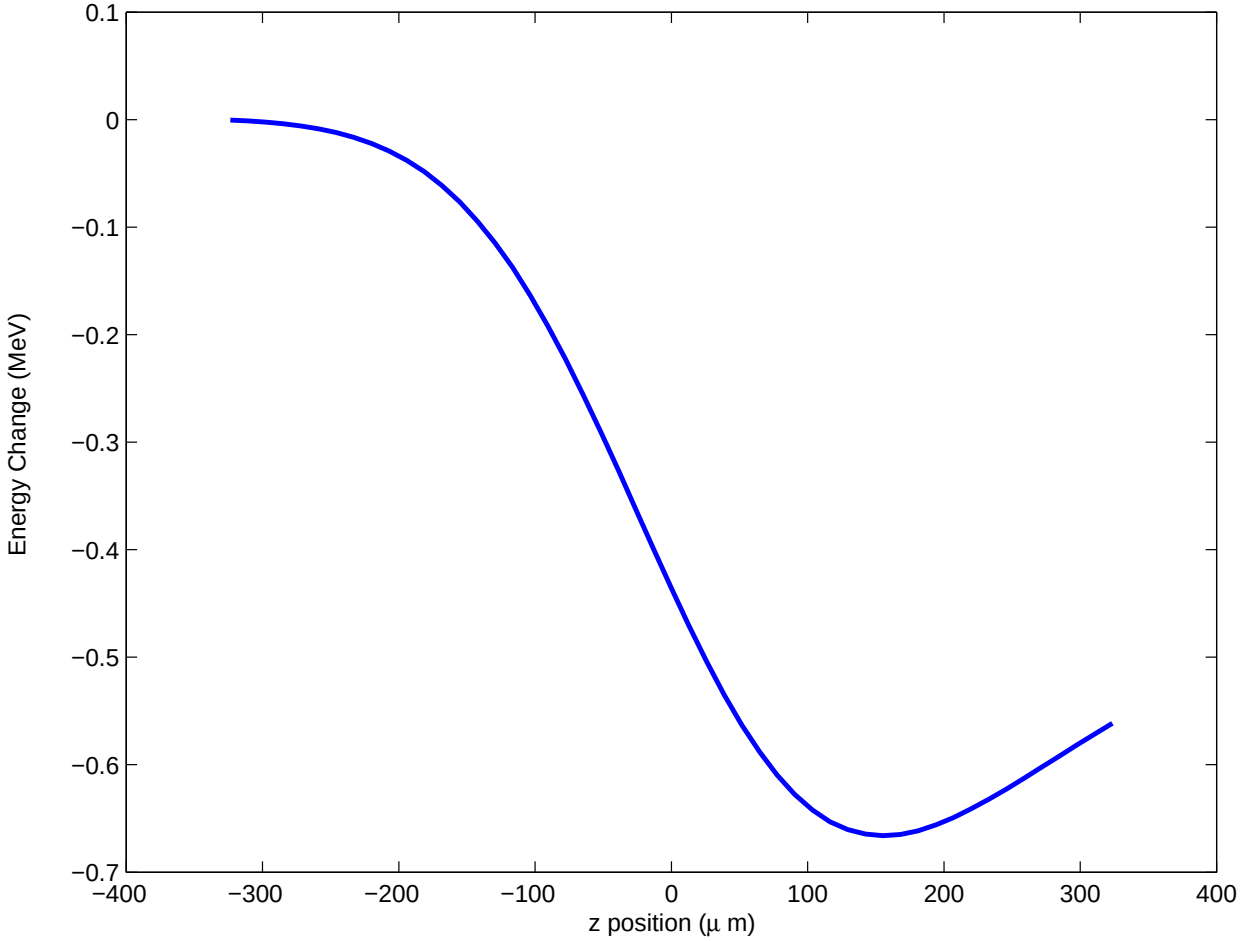

Figure 2: Energy loss versus z position for an NLC bunch (1.2 nC, 110 μm RMS length, 3 σ_z truncation) in an NLC 60 cm RF structure. The beam head corresponds to $z < 0$.

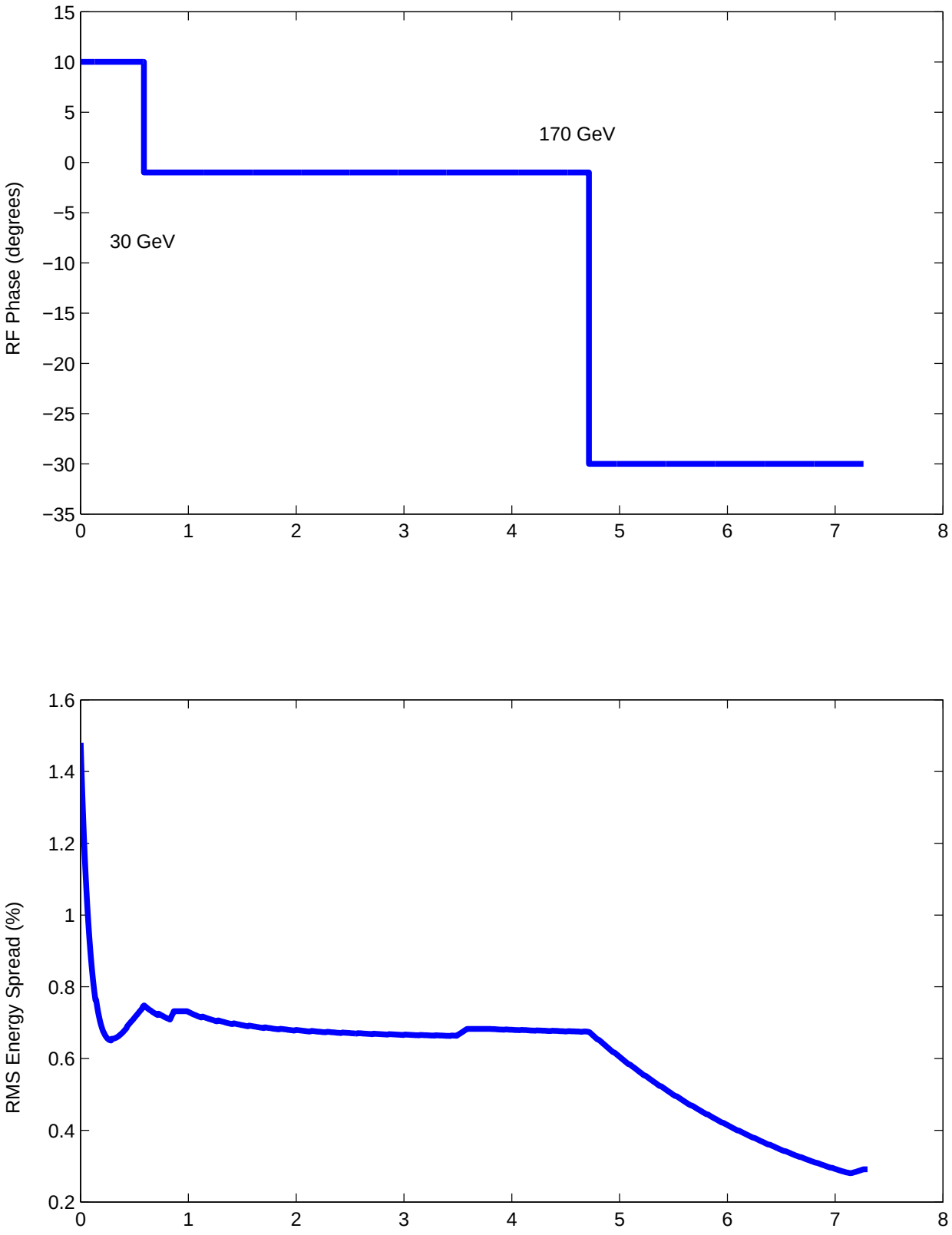

Figure 3: RF phase (top) and RMS energy spread (bottom) versus s for the NLC main linac in nominal BNS configuration. Energy spread includes 1.48% incoming energy spread.

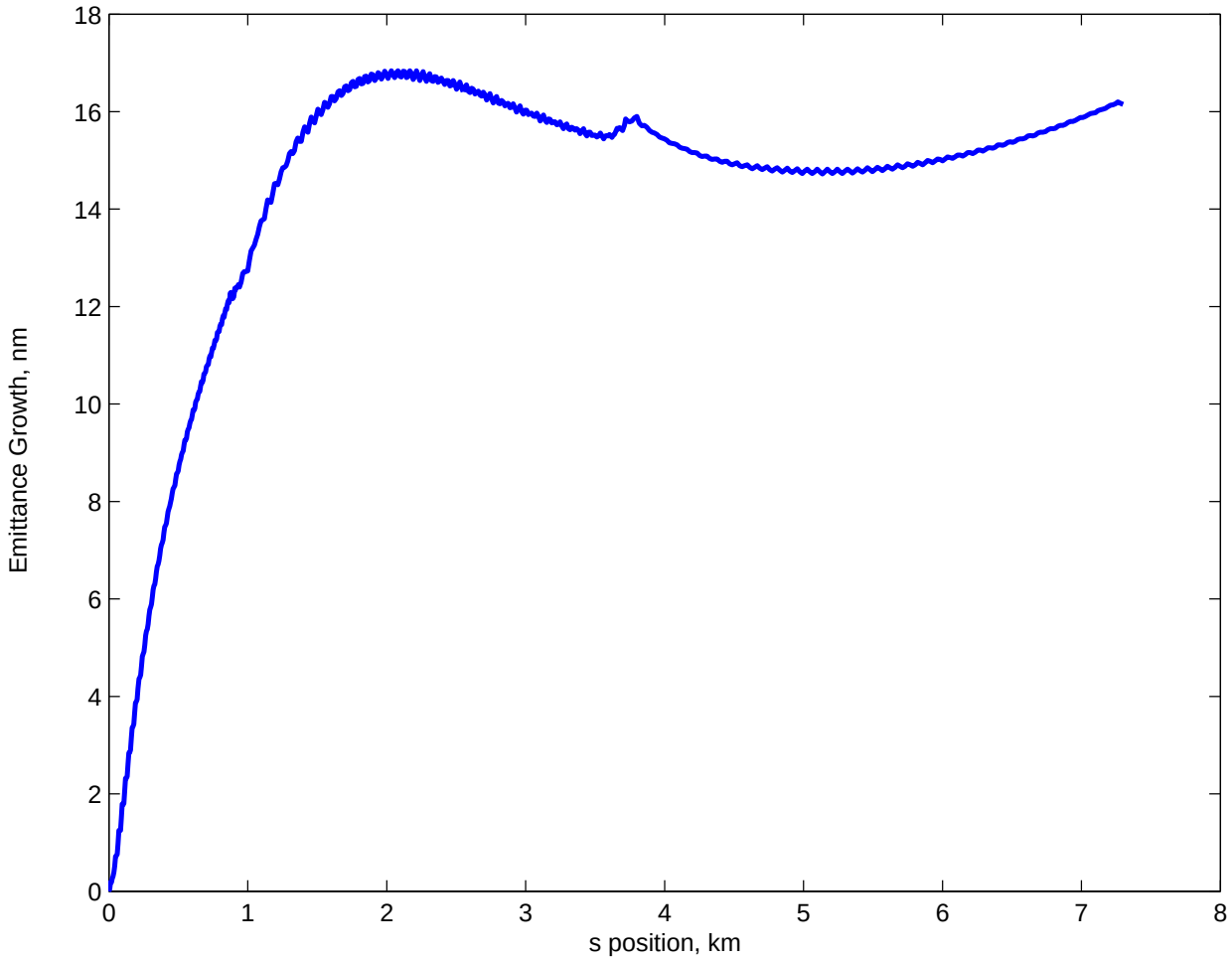

Figure 4: Emittance growth versus s position for 1 σ_y initial offset, nominal BNS configuration. The incoming emittance is 20 nm.

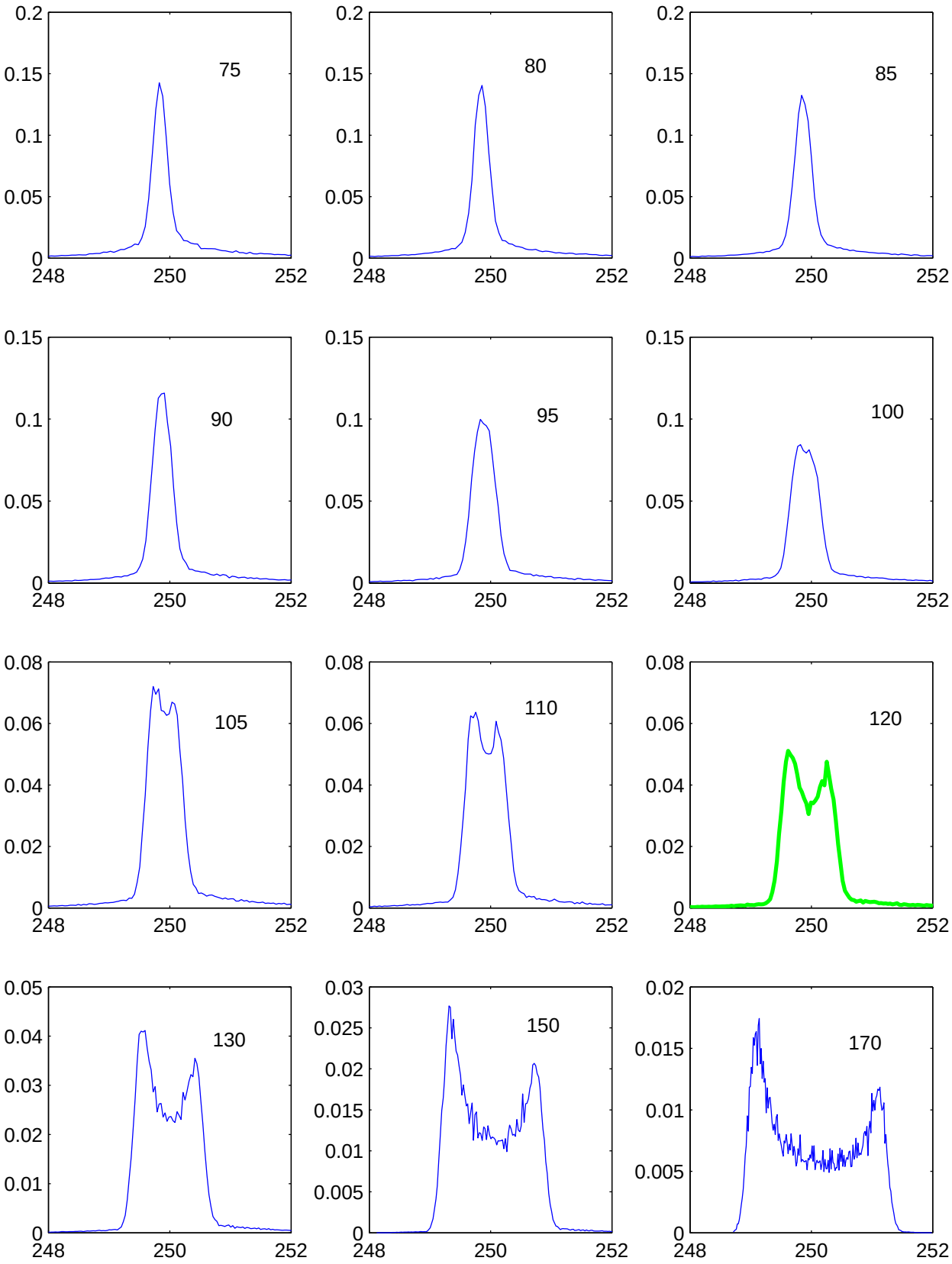

Figure 5: Spectrum of the beam at the end of the NLC linac for various final switch energies. New optimal case (final switch at 120 GeV) is in green. Nominal case is 170 GeV final switch point.

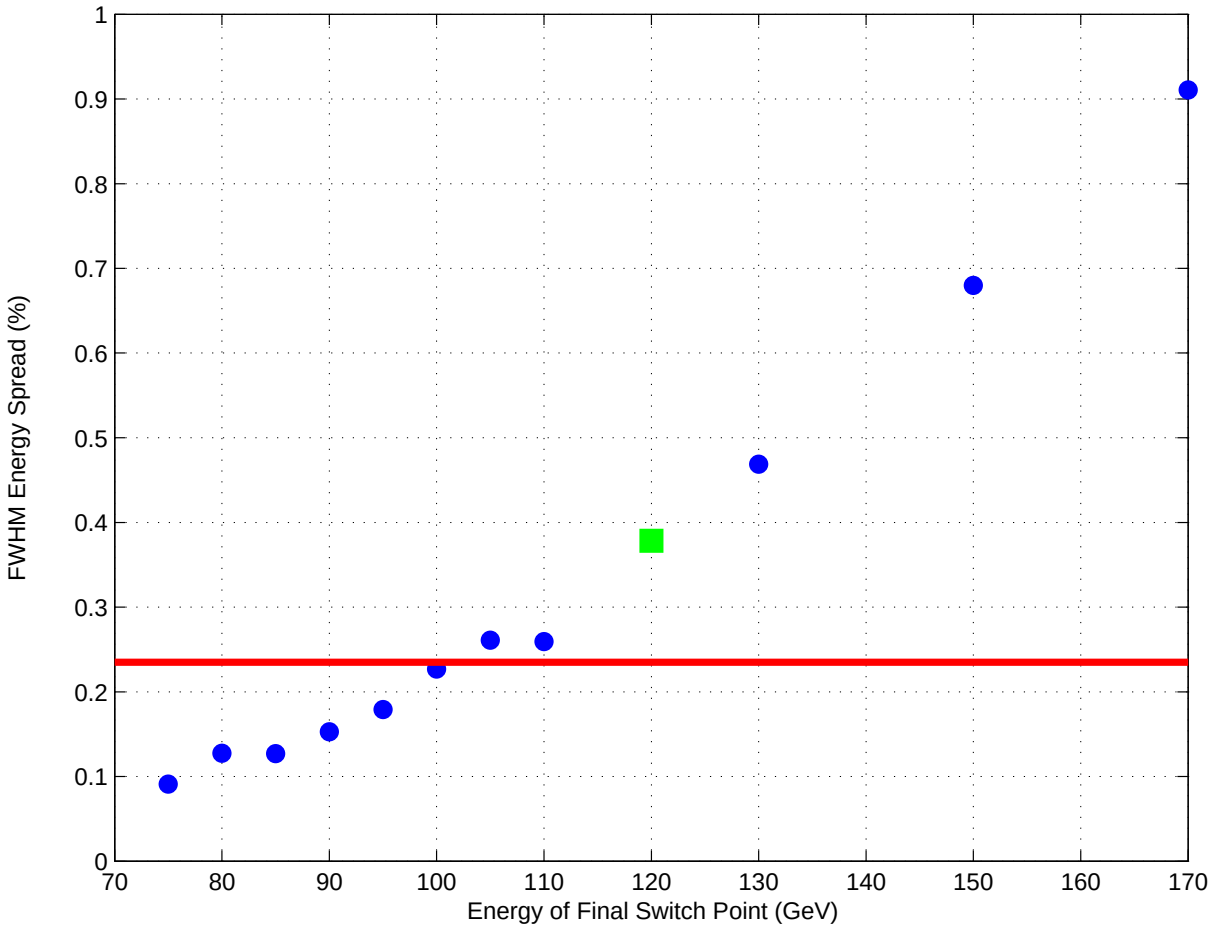

Figure 6: Full width at half maximum energy spread, NLC beam at the end of the linac for various final energy switches. The FWHM of the TESLA beam is also shown for comparison (red line).

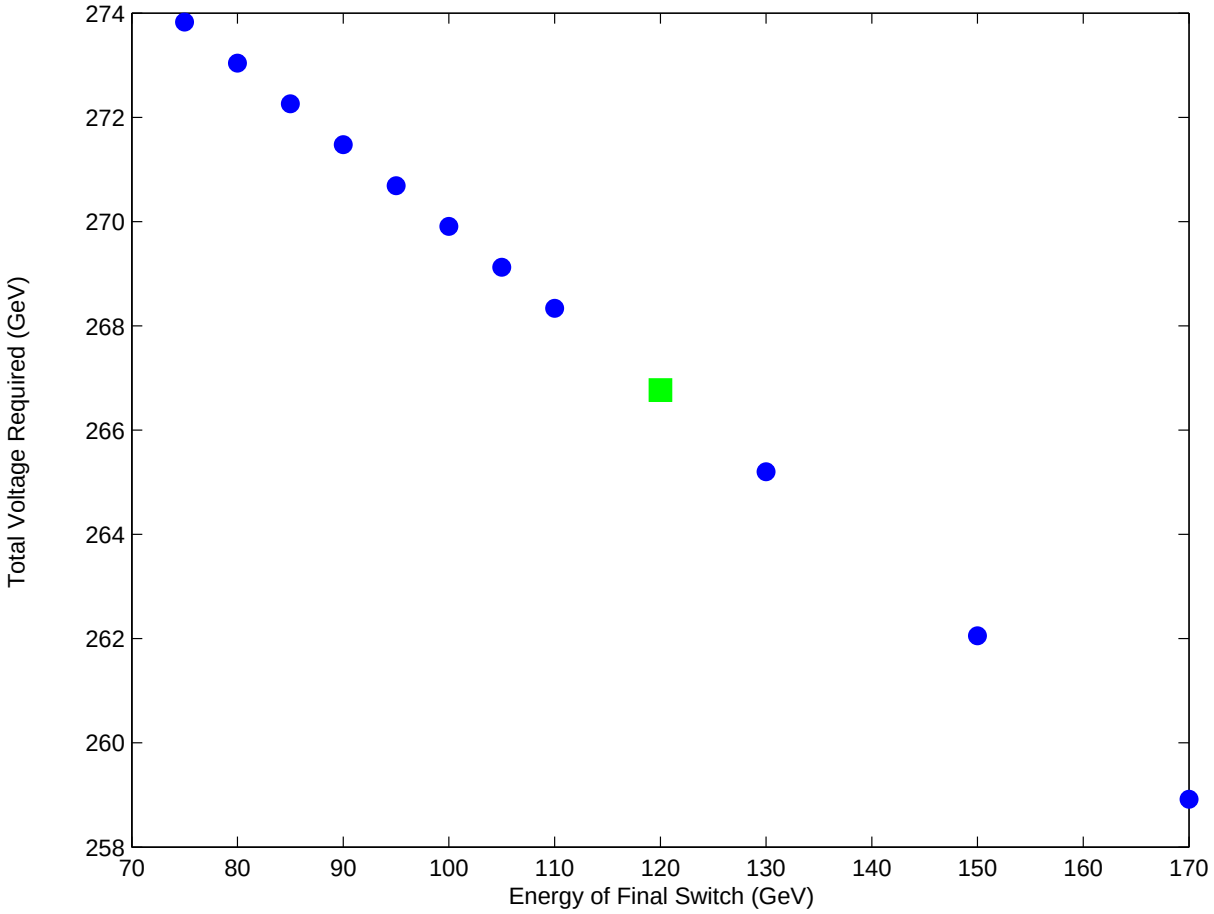

Figure 7: Total accelerating voltage required to achieve 250 GeV beam energy for various final energy switch points.

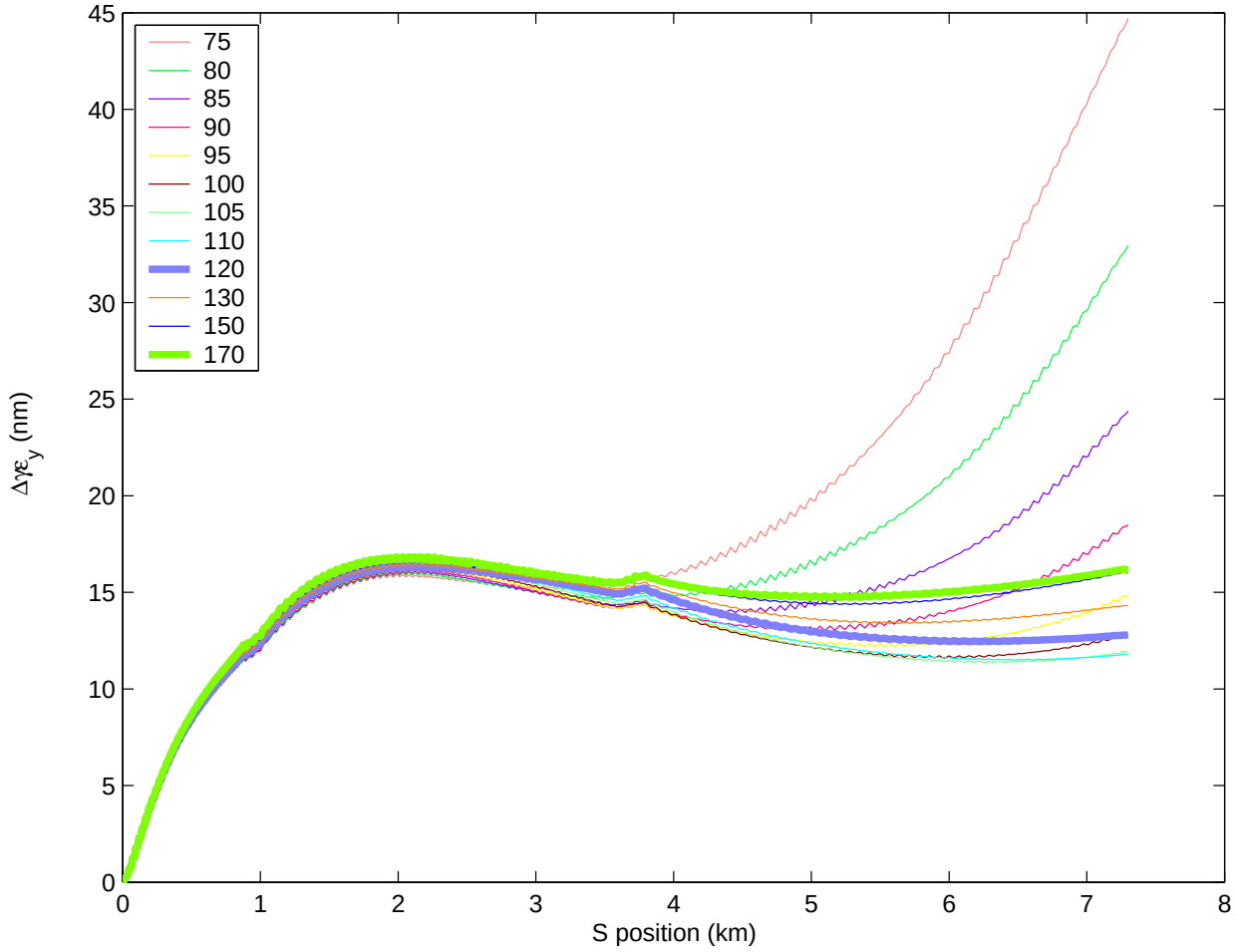

Figure 8: Emittance growth versus s for a 1 σ_y initial offset, various final switch energies. Nominal and new optimal cases are indicated by thicker lines.

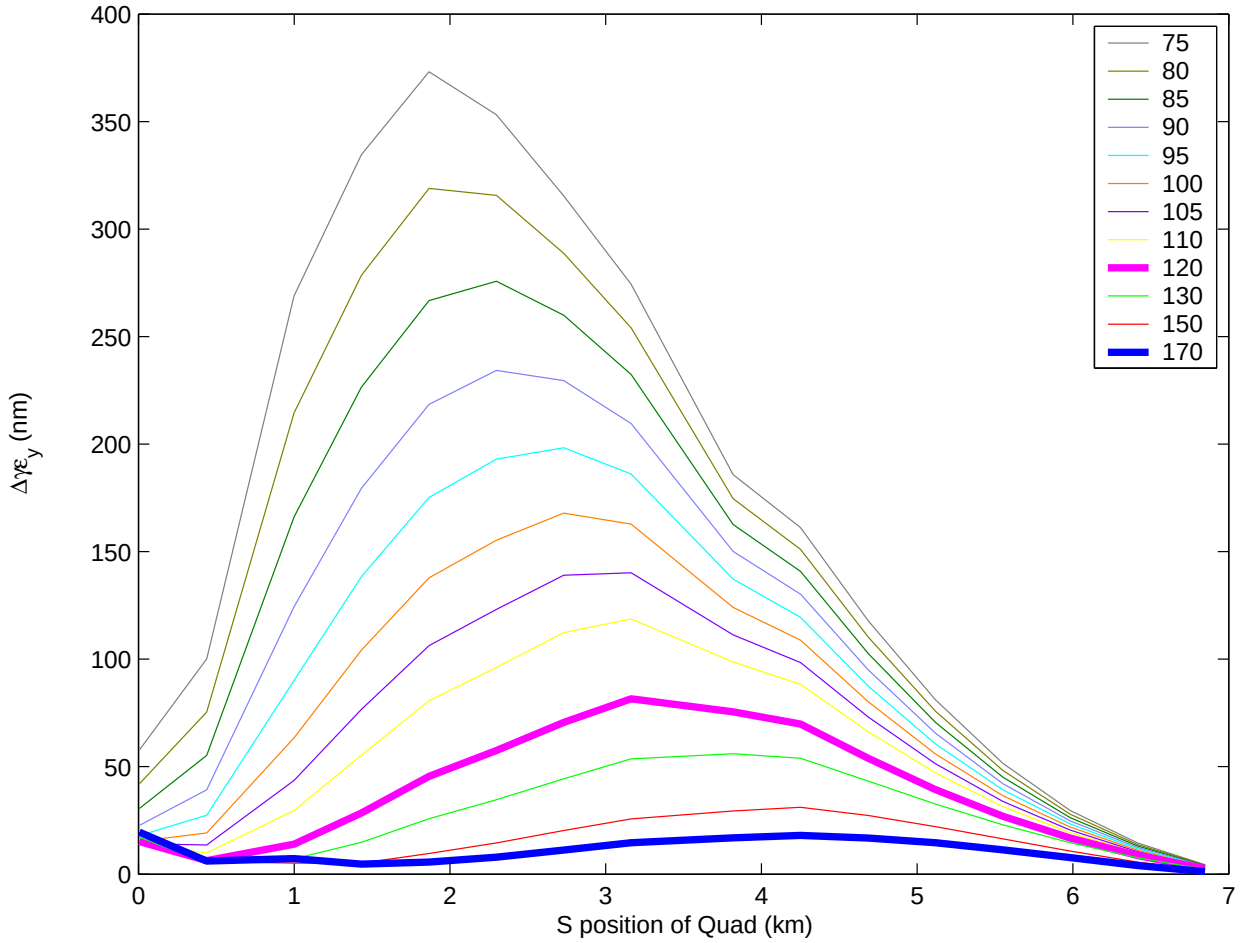

Figure 9: End-linac emittance growth for 1 μm offsets of various quads in the linac, various final energy switch points, plotted as a function of the quadrupole s position. Nominal and new optimal cases are indicated by thicker lines.

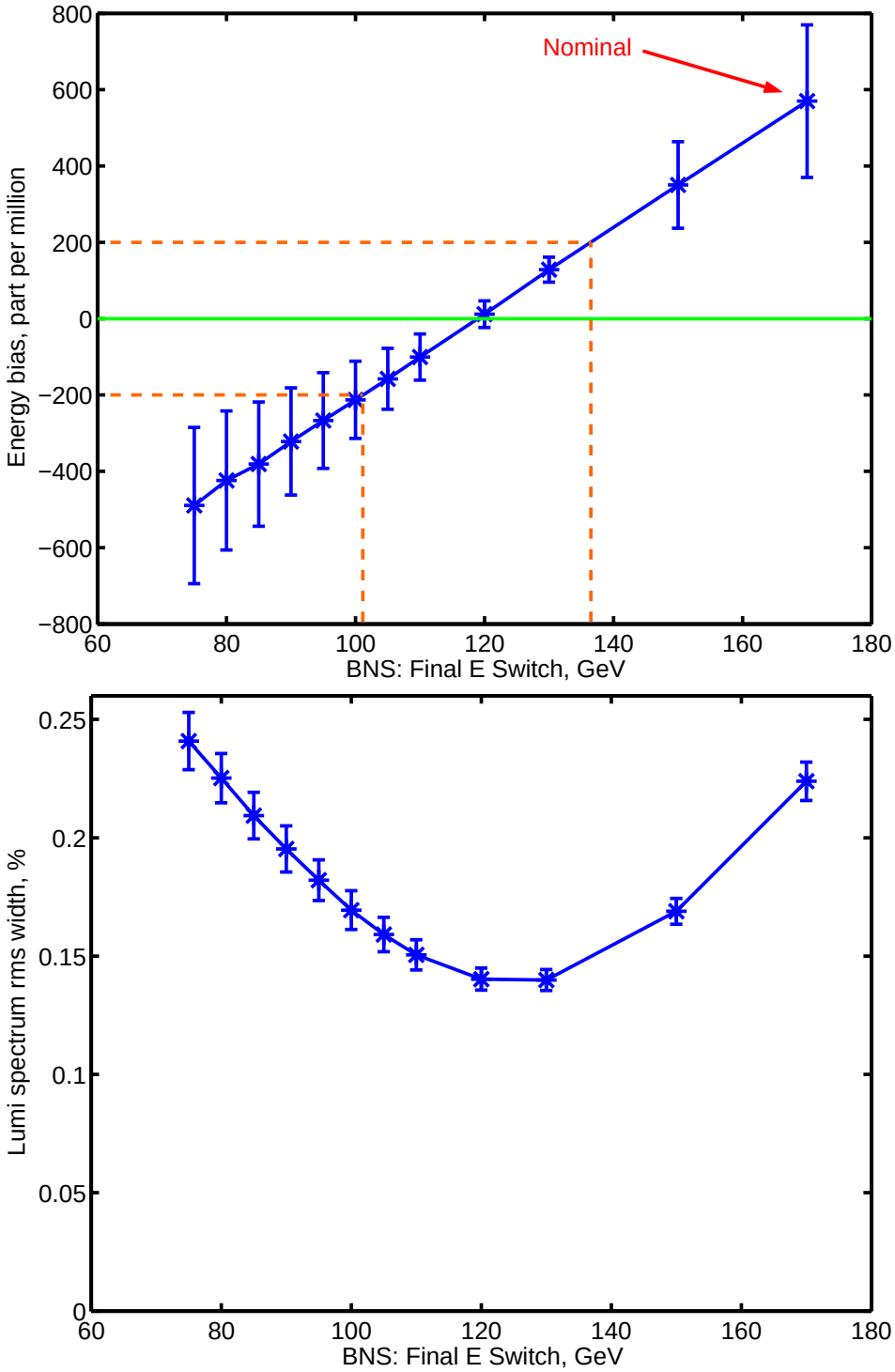

Figure 10: Energy bias and rms width of the luminosity spectrum versus final energy switch of BNS in the linac. Simulations for 6 realistic files of beam IP distribution. Obtained with Guinea-Pig beam-beam program with beamstrahlung switched off.

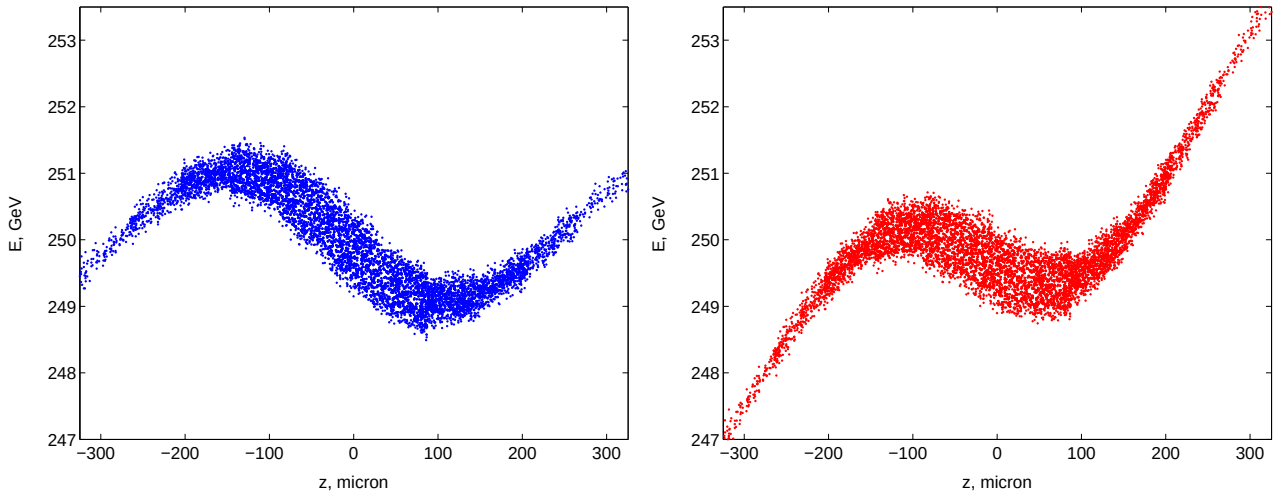

Figure 11: Energy - Z distribution of the NLC beams. Left nominal BNS case. Right new BNS configuration which minimizes the energy bias and the width of the luminosity spectrum. Bunch head is at $z < 0$.

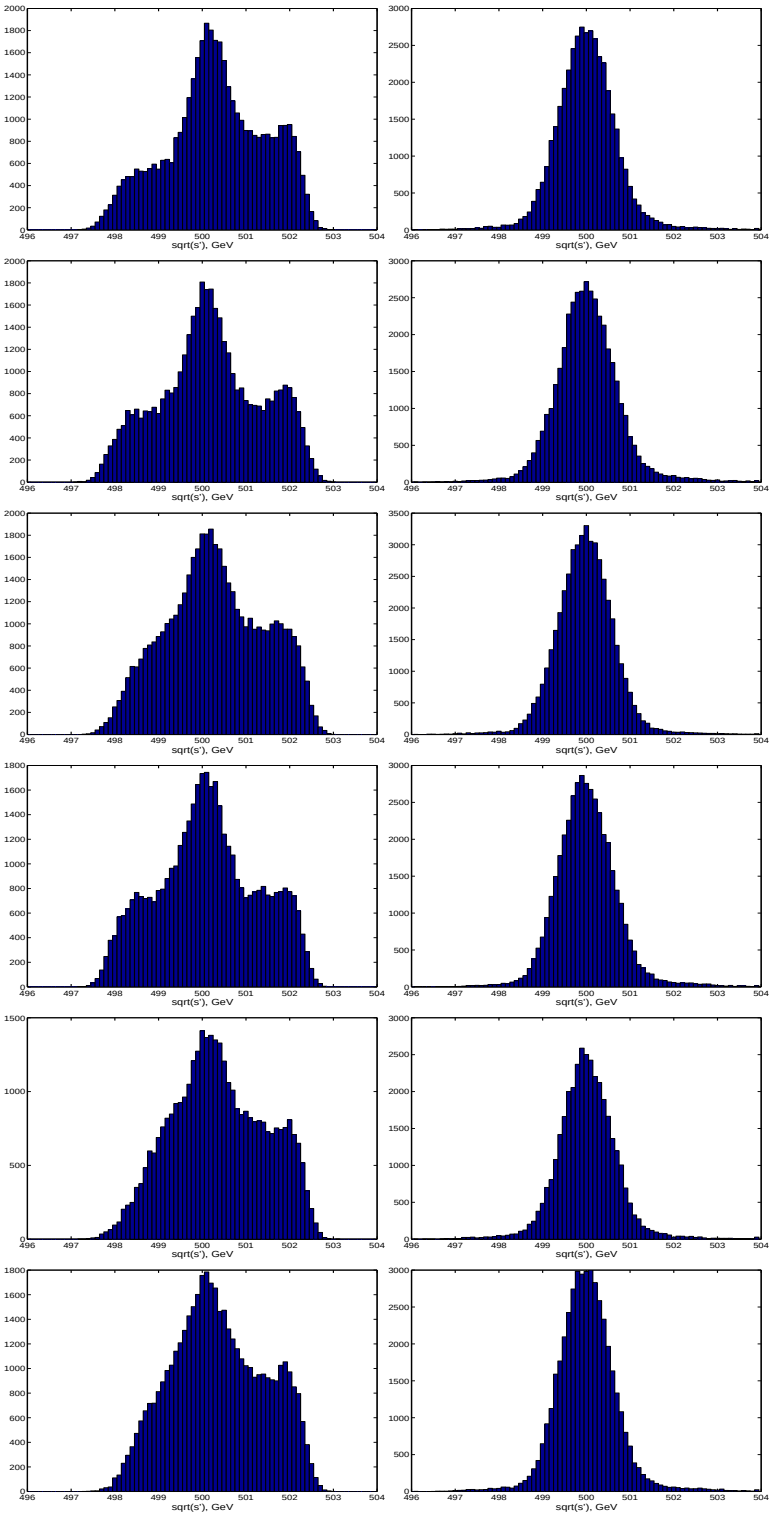

Figure 12: Luminosity spectrum for six different realistic files of beam IP distribution (correspond to different misalignment seeds in the linac). Left - nominal BNS case. Right - new BNS configuration which minimize energy bias and luminosity spectrum width. Beamstrahlung is switched OFF.

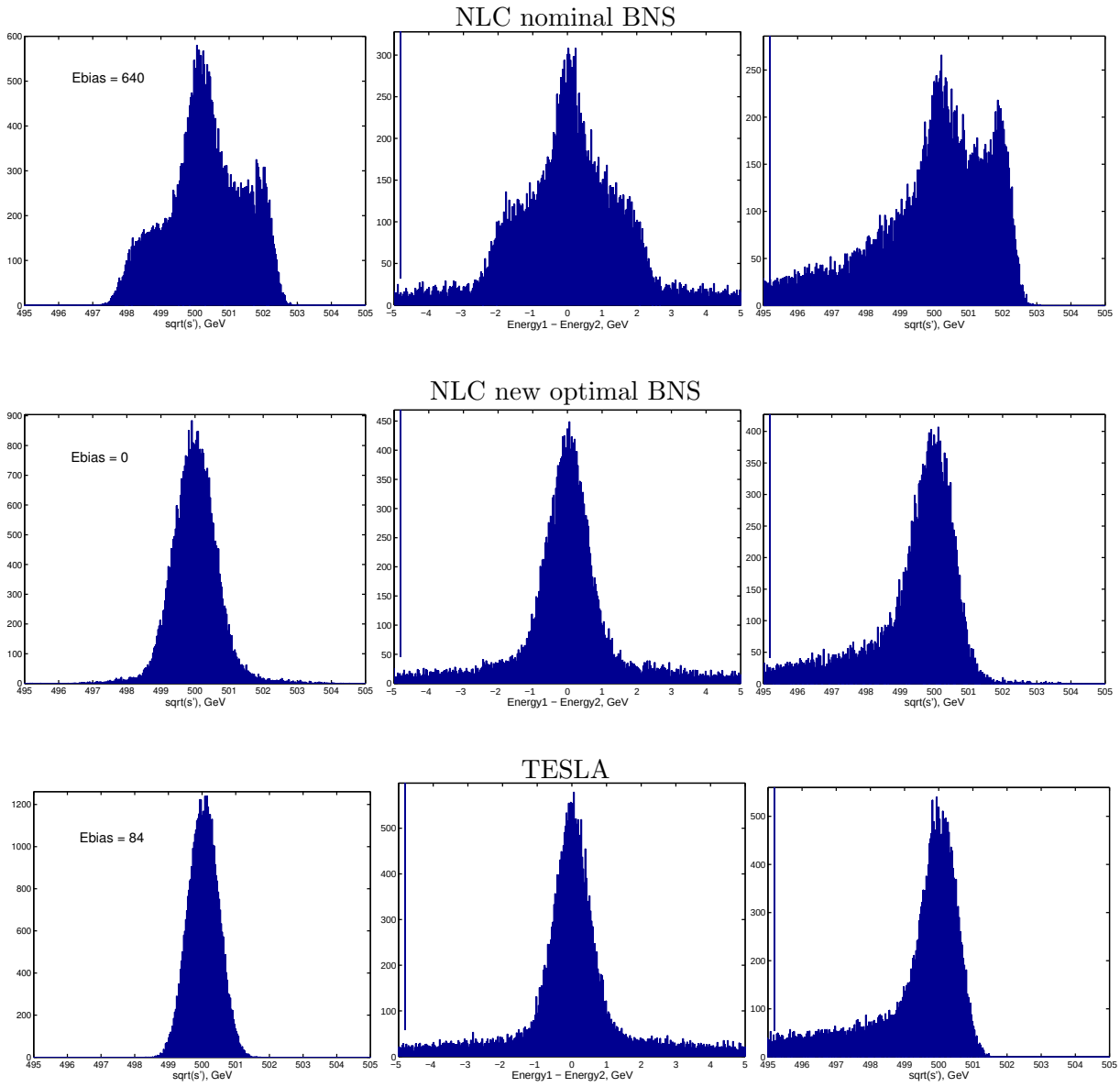

Figure 13: Luminosity spectra in NLC with nominal BNS and with new optimal BNS, and in TESLA. Beamstrahlung is switched OFF (left column) and ON (middle and right columns).

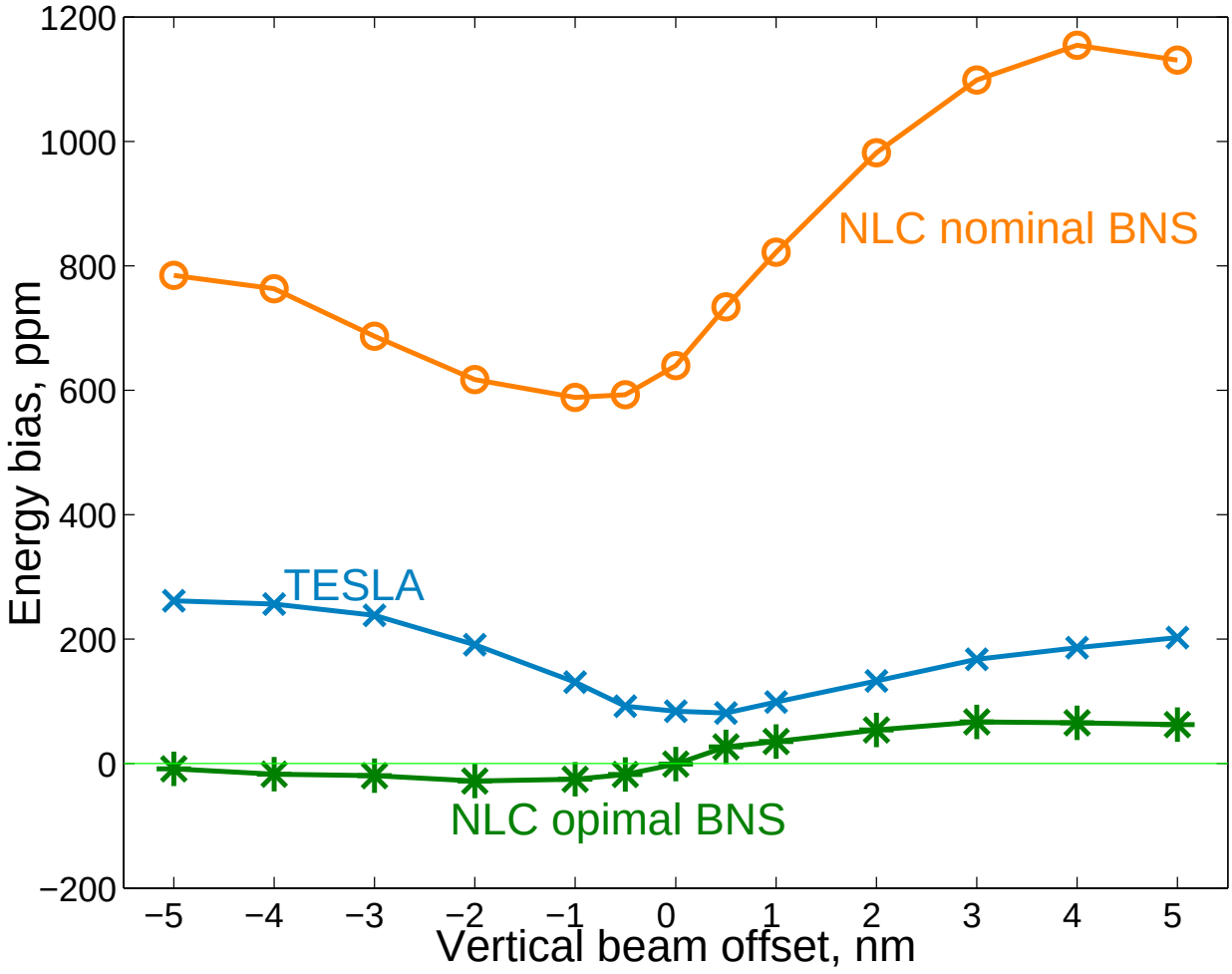

Figure 14: Sensitivity of the energy bias to the vertical offset of the beams.